Controlling chaotic states of a Pierce diode

Holger Friedel, Rainer Grauer, and Karl H. Spatschek
Institut für Theoretische Physik, Heinrich–Heine–Universität Düsseldorf
D–40225 Düsseldorf, Germany
(February 24, 1998)

A recently developed nonlinear approach to control chaos is applied to the Pierce diode. In the latter, both (kinetic) virtual cathode oscillations and (hydrodynamic) plasma oscillations appear. Via the period doubling route, the plasma oscillations can become chaotic. They are, however, usually superimposed by virtual cathode oscillations. Here it is shown that in the hydrodynamic as well as in the kinetic regime unstable periodic orbits can be stabilized. The results can be applied to bring the Pierce diode into a well–defined state of microwave oscillations.

I. INTRODUCTION

Nonlinear dynamics has demonstrated that even simple systems (i.e. systems modeled by relatively simple equations of motion, as for example maps or nonlinear ordinary differential equations) may exhibit very complicated dynamics. This behavior, now well known as deterministic chaos, can be found in many situations of mathematical physics (and beyond that in chemical, biological, and even ecological systems). Important in this context is the fact that such systems lack the possibility of predicting their long time behavior. Therefore, one tries to find ways of preventing chaos. Ott, Grebogi and Yorke [1] have shown that chaotic systems may be controlled by making only small changes in an accessible parameter. Their key observation was that an infinite number of unstable periodic orbits are embedded in chaotic attractors. Due to ergodicity, the trajectory will visit any neighborhood of one of these orbits in a finite time. One then changes the control parameter in such a way that the unstable orbit is stabilized. As Ott, Grebogi and Yorke (OGY) have shown, this can be achieved by the well–established technique of pole assignment which goes back to the 19th century (see e.g. the posthumously published textbook by LaSalle [2]).

During the last years, many aspects of controlling chaos have been investigated. Out of them we would like to mention only the following two which are most relevant for the present paper. First, the perhaps more technical aspect of nonlinear control. Based on center manifold theory it was possible [3] to generalize the otherwise linear control rules to nonlinear ones. This helps to enlarge the accessible part of the phase space. The second aspect concerns the dimensions of the systems. Besides maps and systems of nonlinear ordinary differential equations, also systems with infinite degrees of freedom can be controlled. In the mathematical sense this means that we can control dynamic systems of (a set of) partial differential equations. This is very important for physical applications, i.e. experiments. In the following we shall demonstrate an effective control for the Pierce diode (which in the mathematical sense is represented by an infinite dimensional, continuous system of differential equations). In physical terms, the Pierce diode can be understood as a prototype of a bounded plasma device.

The theory of bounded plasmas has a long tradition. In 1944 J.R. Pierce introduced an idealized model of a thermionic discharge plasma [4]. His model improved the classical plasma oscillation model of Tonks and Langmuir [5] by introducing physically motivated boundary conditions. Hereby, new instability mechanisms have been found which may act as a source of plasma oscillations. Thus, the model represents an important step towards a quantitative description of bounded plasma systems. A comprehensive introduction into the field can be found in a recent overview by Kuhn [6]. In the following, we shall focus on results concerning the motivation and understanding of dynamical chaos control in the Pierce diode.

The Pierce diode is a one–dimensional collisionless model. It consists of two short–circuited electrodes with fixed electric potential $\phi(0) = \phi(L) = 0$, where L is the system length. It is assumed that at the cathode (spatial variable $x = 0$) a mono–energetic electron–beam with velocity $v(0) = v_0$ and charge density $\rho(0) = -\rho_0$ is injected. The electrons move in a fixed homogeneous ion background of density ρ_0 and are absorbed at the anode ($x = L$). Thus, in the case of a homogeneous electron beam ($\rho \equiv -\rho_0$) the system is quasi–neutral. A linear stability analysis of the trivial solution $\rho = -\rho_0$ and $v = v_0$ shows that due to the boundary conditions the homogeneous state is unstable for most values of the Pierce parameter (see below) $\alpha > \pi$. At odd multiples of π a non–oscillating mode is getting unstable when α is increased [4]. This effect is now well known as the classical Pierce instability. Later, a second instability has been found by Cary and Lemmons [7], known as the oscillatory Pierce instability. They found that in small α–regions below odd multiples of π the homogeneous state is stable. When further decreasing α, a pair of modes with complex conjugate eigenvalues is becoming unstable. The smallest α–value where this happens is $\alpha \approx 9.1$. Both instability mechanisms lead to completely different nonlinear dynamical behaviors. While the classical Pierce instability leads to inhomogeneous states or to virtual cathode relaxation oscillations (depending on the initial conditions), we get stable limit cycles in the oscillatory case. When further decreasing α these limit cycles become unstable, too, and after a period doubling cascade chaotic oscillations occur. The strongly nonlinear virtual cathode oscillations ultimately require a kinetic description, while for the plasma oscillations one can use a hydrodynamic description in a broad regime. When controlling in the following both of them, we apply different techniques in the hydrodynamic and the kinetic regimes, respectively.

Both instabilities have been examined by various authors. With respect to the nonlinear developments of the instabilities, two remarks may characterize the present situation. First, in the oscillatory case, up to now the best analytical approach is the three mode Galerkin approximation of Hörhager and Kuhn [8] for periodic solutions. Galerkin approximations quite often show different behaviors than the original system [9]. When compared to numerical simulations, the results of Hörhager and Kuhn are very encouraging. However, there remains the open question of the analytical theory for the transition to and the stability of limit cycles. When accepting the common picture of instability and period doubling route to chaos, the problem arises to control the appearing chaos. Secondly, in the unstable case leading to virtual cathode oscillations, no analytical theory is available, and numerical simulations are state of the art. When addressing the question of suppressing the (nonlinear) virtual cathode oscillations, we shall also rely on numerical methods. In addition, it should be mentioned that although theoretically the regions of plasma oscillations and virtual cathode oscillations are well–separated, in practice (experiment) it is very difficult to get access to a region of plasma oscillations without virtual cathode oscillations. Thus our first aim will be a prescription to suppress the virtual cathode oscillations. Starting with the resulting quenched states we shall look for appearance and control of plasma oscillations in the chaotic regime. As has been mentioned already, that result will be important for microwave generation.

The paper is organized as follows. In Sec. II, we present the hydrodynamic model and briefly review the classical Pierce instability as well as the oscillatory instability. An analytical theory (normal forms) for the first bifurcating states is presented. In case of the classical Pierce instability, leading to virtual cathode oscillations, the hydrodynamic model breaks down before saturation. Therefore, a numerical subsection dealing with (numerical) solutions in the kinetic regime is enclosed. The advantages of a symplectic integrator are described, being helpful for the later suppression of virtual cathode oscillations. The controlling of the Pierce diode is presented in Sec. III. After a brief summary of the general nonlinear control technique, we first suppress virtual cathode oscillations, since the latter have the tendency to conceal (at least experimentally) the other phenomena we are interested in. After successfully suppressing virtual cathode oscillations we present detailed results on controlling hydrodynamic (plasma) oscillations in the chaotic regime. The procedure can be used to bring the Pierce diode into a state of pure microwave oscillations. The paper is concluded by a short summary and discussion.

II. NONLINEAR STATES OF THE PIERCE DIODE

A. Analytical theory for the first bifurcation

As long as the velocity distribution is single valued, the Pierce diode may be described by the standard set of fluid equations for the electrons [4], namely the equation of continuity for the electron charge ρ,

$$\partial_t \rho + \partial_x (v\rho) = 0 \quad , \tag{2.1}$$

and the momentum balance for the velocity field v (Euler equation)

$$\partial_t v + v\partial_x v = \frac{e}{m_e}\partial_x \phi \quad , \tag{2.2}$$

where the electric potential ϕ is determined self–consistently by Poisson's equation

$$\partial_{xx}\phi = -\frac{1}{\epsilon_0}(\rho_0 + \rho) \quad . \tag{2.3}$$

Here e is the elementary charge, m_e is the electron mass at rest, and ϵ_0 is the vacuum permittivity. In their dimensionless form, these equations depend only on one dimensionless parameter

$$\alpha = \frac{\omega_p L}{v_0} \quad , \tag{2.4}$$

the so called Pierce parameter, where $\omega_p = [e\rho_0/(\epsilon_0 m_e)]^{\frac{1}{2}}$ is the electron plasma frequency. One should note that the original definition of α by Pierce is slightly different.

Without going into the details, we should repeat that a linear stability analysis shows two types of instabilities. The initial stages of both instabilities can be described by the hydrodynamic model presented above. The hydrodynamic model will remain good for plasma oscillations in a wide parameter regime. On the other hand, the nonlinear theory of the virtual cathode oscillations requires a kinetic treatment.

Let us now develop the nonlinear theory for the first bifurcation from the homogeneous state. During the last years center manifold theory became a standard tool for studying the nonlinear bifurcation behavior of systems near the onset of instability. This perturbation theory is based on the concept of invariant manifolds and thus gives a very clear geometrical picture of the dynamical behavior of the system. A very brief summary of the basic results of center manifold theory is as follows. Consider the system of differential equations

$$\dot{a} = Aa + N(a,b), \quad a \in R^n, \tag{2.5}$$
$$\dot{b} = Bb + M(a,b), \quad b \in R^m, \tag{2.6}$$

where the eigenvalues of the matrix A are assumed to have a vanishing real part, and those of B are assumed to have real parts strictly less than 0. Center manifold theory states that there exists a manifold (the center manifold which is tangential to the eigenspace spawned by the eigenvectors of A) on which the asymptotic long time dynamics takes place, if initial conditions are in a sufficiently small neighborhood of the zero solution. That means that the dimensionality of the problem can be reduced from $n+m$ to n. In addition, the center manifold is smooth and can therefore locally be described as a graph of some function h. Knowing this function h, the long time dynamics is governed by

$$\dot{a} = Aa + N(a, h(a)) \quad , \tag{2.7}$$

which means that the stable components b are slaved by the marginal modes a (reduction principle). The rate of how solutions are attracted by the center manifold is related to the eigenvalue of the least damped stable mode.

If parameters $c \in R^l$ are present, the parameter dependences of the solutions can be studied by enlarging the center manifold according to

$$\dot{a} = Aa + N(a,b,c) \quad , \tag{2.8}$$
$$\dot{c} = 0 \quad , \tag{2.9}$$
$$\dot{b} = Bb + M(a,b,c) \quad . \tag{2.10}$$

More details can be found in the books of Carr [10] and Chow and Hale [11]. Examples for partial differential equations are reported in [12].

By applying center manifold theory to our problem, we derived both, the normal forms for the classical Pierce instability and for the oscillatory case. The normal forms are the equations of motion for the amplitude a_1 of the marginal mode, following from the reduction principle. Since several technical aspects are involved here, we only present the final results. A detailed derivation can be found in [13].

In the classical case we get the normal form of a transcritical bifurcation:

$$\dot{a}_1 = -\frac{\pi^2 \Delta v}{4} a_1 - \frac{\pi}{2} a_1^2 \quad . \tag{2.11}$$

Here we used a variation Δv of the boundary condition for $v(0)$ as the control parameter; Δv is related to the Pierce parameter by $\alpha = \alpha_0/(1+\Delta v)$. Clearly, α_0 is the value of α for $\Delta v = 0$. This bifurcation is also known as the "exchange of stability" which will become clear in the following discussion. Equation (2.11) has two stationary solutions (fixed points): $a_1 = 0$, which corresponds to the homogeneous state, and $a_1 = -\pi\Delta v/2$, corresponding to an inhomogeneous equilibrium. For $\alpha < \pi$ ($\Delta v > 0$), the homogeneous state is stable while the inhomgeneous state is unstable, as illustrated in Fig. 1. For $\alpha > \pi$, the fixed points "exchange" their stability behavior – now the homogeneous state is unstable and the inhomogeneous state is stable. This gives us already some insight into the possible nonlinear dynamics. For $\alpha > \pi$, perturbations of the homogeneous state with positive amplitudes a_1 in the unstable mode will start growing and saturate in the inhomogeneous equilibrium. For $a_1 < 0$, our (local) theory does not predict a saturation. Here, the unstable mode grows until the hydrodynamic model breaks down, and virtual cathode oscillations occur.

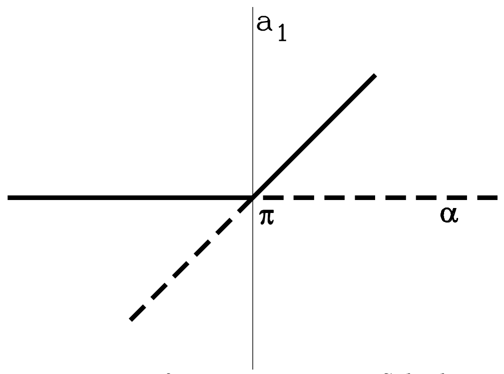

FIG. 1. Exchange of stability at $\alpha = \pi$. Solid lines indicate stability, dashed lines instability.

Another interesting aspect is the appearance of virtual cathode oscillations also for $\alpha < \pi$, where the homogeneous solution is stable. These cathode oscillations were first observed by Lawson [14]. Theoretically, the phenomenon can be understood as the instability of the homogeneous state against perturbations of finite amplitudes. If the system is perturbed in such a way that the trajectory is "kicked" to the far side of the inhomogeneous solution ($a_1 < -\pi\Delta v/2$), we get no saturation in our local theory. Again, one observes virtual cathode oscillations. This is a typical threshold effect which can be induced by applying a random force to the system. Similar behaviors can be observed, e.g., in dynamical systems containing a saddle–node. There, such perturbations sometimes lead to partly periodical behavior (see e.g. [15]), as is the case here, purchasing this effect the name stochastic resonance.

The situation is much more complicated in the oscillatory case . There the marginal modes are not Fourier modes. The *complex* wave numbers are given implicitly by a transcendental equation [4]. Thus, we have to determine the coefficients in the equation of motion for the complex amplitude a_1 (of one of the complex conjugate pair of modes),

$$\dot{a}_1 = (A_1^1 + A_1^{13}\Delta v) a_1 + A_1^{11\bar{1}} |a_1|^2 a_1 \ , \tag{2.12}$$

numerically. The numerical values of the coefficients are as follows: $A_1^1 \equiv i\omega_0 = i1.70405$, $A_1^{13} = 14.2893 - i5.82798$, $A_1^{11\bar{1}} = -5.31462 + i3.30359$. Equation (2.12) is the normal form for a supercritical Hopf bifurcation.

It explains the occurrence of stable limit cycles near the onset of instability. The typical scenario of a Hopf bifurcation is schematically represented in Fig. 2. For values of α above the bifurcation point at $\alpha_c = 9.10000033...$ the homogeneous state is stable. Below the bifurcation point the complex conjugate pair of eigenmodes becomes unstable. In its long time behavior the system saturates in a periodic solution (limit cycle).

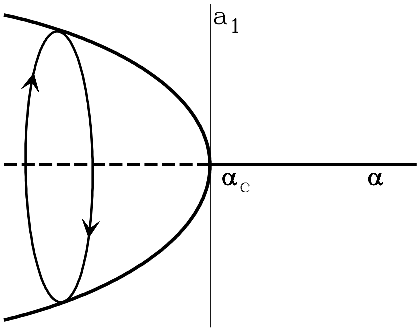

FIG. 2. Hopf bifurcation at $\alpha = \alpha_c$.

The introduction of polar coordinates ($a_1 = re^{i\varphi}$), enables us to calculate the saturation amplitude $r^2 = -\operatorname{Re} A_1^{13} / \operatorname{Re} A_1^{11\bar{1}} \Delta v$ and the (nonlinear) frequency $\dot{\varphi} = \operatorname{Im}(A_1^1 + A_1^{13}\Delta v + A_1^{11\bar{1}} r^2)$ of the limit cycle. The typical square root dependence of the saturation amplitude is illustrated in Fig. 2. As shown in Fig. 3, the theoretical results are also in pretty good quantitative agreement to our numerical studies (that reproduce the results of Godfrey [16] and Lawson [14]). There it is shown, that the prediction error of the theoretically determined frequency of the limit cycle is less than one percent.

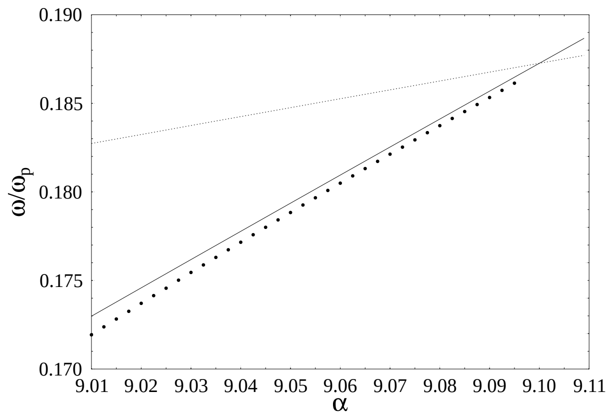

FIG. 3. Comparison of the numerically determined frequency (filled circles) with theoretical predictions from nonlinear theory (solid line). For illustration, we have also included the linear frequency (dotted line).

B. Numerical methods for virtual cathode oscillations

There are different possibilities of modeling the Pierce diode numerically. Perhaps, the most obvious way is using a finite difference scheme for the hydrodynamic model equations, namely standard upwind differencing [17]. Unfortunately, the hydrodynamic model is not capable of simulating kinetic effects as virtual cathode oscillations. Therefore we developed a symplectic particle in cell code which models the corresponding Vlasov–Poisson system.

The basic procedure is the numerical integration of the equations of motion for the electrons,

$$\dot{x_i} = v_i \quad , \tag{2.13}$$

$$\dot{v_i} = F_i(\{x_j\}) \quad . \tag{2.14}$$

x_i and v_i are the position and the velocity of the i-th electron, respectively. The force F_i is given self–consistently by Poisson's equation, and hence depends only on the positions $\{x_j\}$ of all electrons. To reduce the computational costs, approximately 10^8 particles are concentrated in one so called macro–particle. Hereby the number of particles is typically reduced to a few thousands.

Although the Pierce diode is a driven and damped nonlinear system, one may regard it as a section of a larger Hamiltonian system where the particles are interacting only in the small area $0 \le x \le L$. This point of view enables us to use a symplectic integration scheme for the time step.

In a symplectic integration scheme one splits the Hamiltonian H into two parts, e.g. the kinetic energy T and the potential energy V. Then, the time development operator $S(t) := e^{t(D_T + D_V)}$ is approximated by products of $e^{\mu_1 t D_T}$ and $e^{\mu_2 t D_V}$, where $D_H z := \{z, H\}$. This idea is strongly connected to the operator splitting method, where in addition symplecticity is preserved. By this procedure we get, e.g., the symmetric second order approximation of $S(t)$,

$$S_2(\Delta t) = e^{\frac{\Delta t}{2} D_T} e^{\Delta t D_V} e^{\frac{\Delta t}{2} D_T} \quad . \tag{2.15}$$

The corresponding symplectic numerical scheme reads

$$x_i^{n+\frac{1}{2}} = x_i^n + \frac{\Delta t}{2} v_i^n \quad , \tag{2.16}$$

$$v_i^{n+1} = v_i^n + \Delta t F_i(\{x_j^{n+\frac{1}{2}}\}) \quad , \tag{2.17}$$

$$x_i^{n+1} = x_i^{n+\frac{1}{2}} + \frac{\Delta t}{2} v_i^{n+1} \quad , \tag{2.18}$$

where n denotes the number of discrete time steps of length Δt. On the first view, this method seems to be more expensive than the leapfrog–scheme which is often used in particle simulations. The great advantage of the present procedure is that higher order schemes can be constructed by products of the second order operator $S_2(t)$, e.g. the fourth order approximation of $S(t)$ is given by

$$S_4(\Delta t) := S_2(\lambda_1 \Delta t) S_2(\lambda_0 \Delta t) S_2(\lambda_1 \Delta t) \quad , \tag{2.19}$$

with $\lambda_0 = -2^{1/3}/(2 - 2^{1/3})$ and $\lambda_1 = 1/(2 - 2^{1/3})$. A detailed derivation of higher order schemes using the Baker–Campbell–Hausdorff formula has been presented by Yoshida [18].

There still remains the problem of calculating the forces. We currently use the standard particle in cell approach [19]. The contribution of the j–th macro–particle to the charge density on a regular grid is approximated by linear weighting according to

$$\rho_i^{(j)} = q_c \frac{(i+1)\Delta x - x_j}{\Delta x^2} \quad , \tag{2.20}$$

$$\rho_{i+1}^{(j)} = q_c \frac{x_j - i\Delta x}{\Delta x^2} \quad , \tag{2.21}$$

where q_c is the charge of one macro–particle, Δx is the grid spacing, and i denotes the index of the l.h.s. nearest neighboring grid point ($x_i \leq x_j < x_{i+1}$). On the regular grid, Poisson's equation is approximated by

$$\phi_{i+1} - 2\phi_i + \phi_{i-1} = -\Delta x^2 \alpha^2 (1 + \rho_i) =: f_i \quad , \tag{2.22}$$

with the boundary conditions $\phi_0 = 0$ and $\phi_N = 0$. This second order difference equation can be solved by the standard ansatz $\phi_i = a_i \phi_{i+1} + b_i$ which reduces the problem to the discrete equation $b_i = a_i(b_{i-1} - f_i)$ where a_i is given by $a_i = i/(i+1)$. The electric field then follows by $E = -(\phi_{i+1} - \phi_{i-1})/(2\Delta x)$. To calculate the forces we use again linear weighting

$$F_j = -\frac{(i+1)\Delta x - x_j}{\Delta x} E_i - \frac{x_j - i\Delta x}{\Delta x} E_{i+1} \quad . \tag{2.23}$$

Our code is implemented in C++. Parts of the code were developed in the context of adaptive mesh refinement for incompressible magnetohydrodynamical flows [20]. An extension to a fully spatio–temporal adaptive treatment similar to [20] seems possible and may be useful when studying singular behavior like virtual cathode formation.

III. CONTROLLING THE PIERCE DIODE

A. Controlling chaos

Before giving a detailed description of chaos control in the Pierce diode, we line out the main principles of the procedure, following Ott, Grebogi and Yorke [1]. Given a deterministic system modeled by a nonlinear map $\mathbf{x}_{n+1} = \mathbf{F}(\mathbf{x}_n, p)$, where $\mathbf{x}_n$ is the system state at "time" n and p is an accessible control parameter, the idea is to stabilize an unstable fixed point embedded in the chaotic attractor for $p = p_0$. It is sufficient to discuss fixed points here, because points of period m are fixed points of the m–th iteration of $\mathbf{F}$. For simplicity we discuss a hyperbolic fixed point with one unstable direction. Due to ergodicity the trajectory visits any small neighborhood of the fixed point in a finite time. In this situation one changes the control parameter p according to

$$p_n = p_0 + \frac{\lambda_u}{\lambda_u - 1} \frac{\mathbf{f}_u \cdot \Delta \mathbf{x}_n}{\mathbf{f}_u \cdot (\mathrm{d}\mathbf{x}_f/\mathrm{d}p)} \tag{3.1}$$

to stabilize the fixed point. Here, λ_u is the unstable eigenvalue, $\mathbf{f}_u$ is the adjoint unstable eigenvector, $\Delta \mathbf{x}_n := \mathbf{x}_n - \mathbf{x}_f$ is the deviation of the trajectory $\mathbf{x}_n$ from the fixed point $\mathbf{x}_f$, and $\mathrm{d}\mathbf{x}_f/\mathrm{d}p$ is the fixed point shift. In control theory, this is known as pole assignment [2]. In the engineering context it appears as Z– or Mellin–transform, where the control law given above has the effect of placing a pole from outside (unstable region) into the inside of the unit circle (stable region) in the complex plane. This control law is only valid in the linear regime of the fixed point when the changes of the control parameter are not too strong. As a consequence, its basin of attraction is limited, leading to sensitivity against noise, which in many practical situations prevents control.

Therefore, we developed a strategy to determine nonlinear control laws, which are much more robust against noise than their linear counterparts and lead to larger attracting regions. Our approach is based on two main ideas and is described in more detail in [3]. First, it is necessary to introduce the control parameter as a dynamic variable ($p \to p_n$). Second, we assume that this dynamical variable belongs to the stable manifold. Center (unstable) manifold theory for maps, which is analogous to the continuous theory discussed above, then says that p_n is a slaved variable. Thus, using the reduction principle, the long time dynamics of the system is guided by the one–dimensional equation of motion on the unstable manifold which can be parameterized by the amplitude of the unstable component u_n. By enforcing the dynamics on the manifold to have the form $u_{n+1} = K u_n$, which is strictly contracting to the fixed point for $|K| < 1$, we were able to determine nonlinear control laws in a constructive way. It turned out that by these laws the basin of attraction of the stabilized fixed points could be significantly enlarged, thereby increasing their Lyapunov stability. Beyond that, it could be shown that in a certain parameter regime these control laws are equivalent to time–delay–feedback. The latter relation is important for an easy implementation of nonlinear control in already existing experiments.

B. Suppressing virtual cathode oscillations

As noted already, the different instabilities in the Pierce diode lead to different nonlinear dynamical regimes. In experimental setups it appears that the regime of virtual cathode oscillations is very dominant. Thus, to control the smooth chaotic oscillations in the hydrodynamic regime, we first have to find a way of suppressing virtual cathode oscillations.

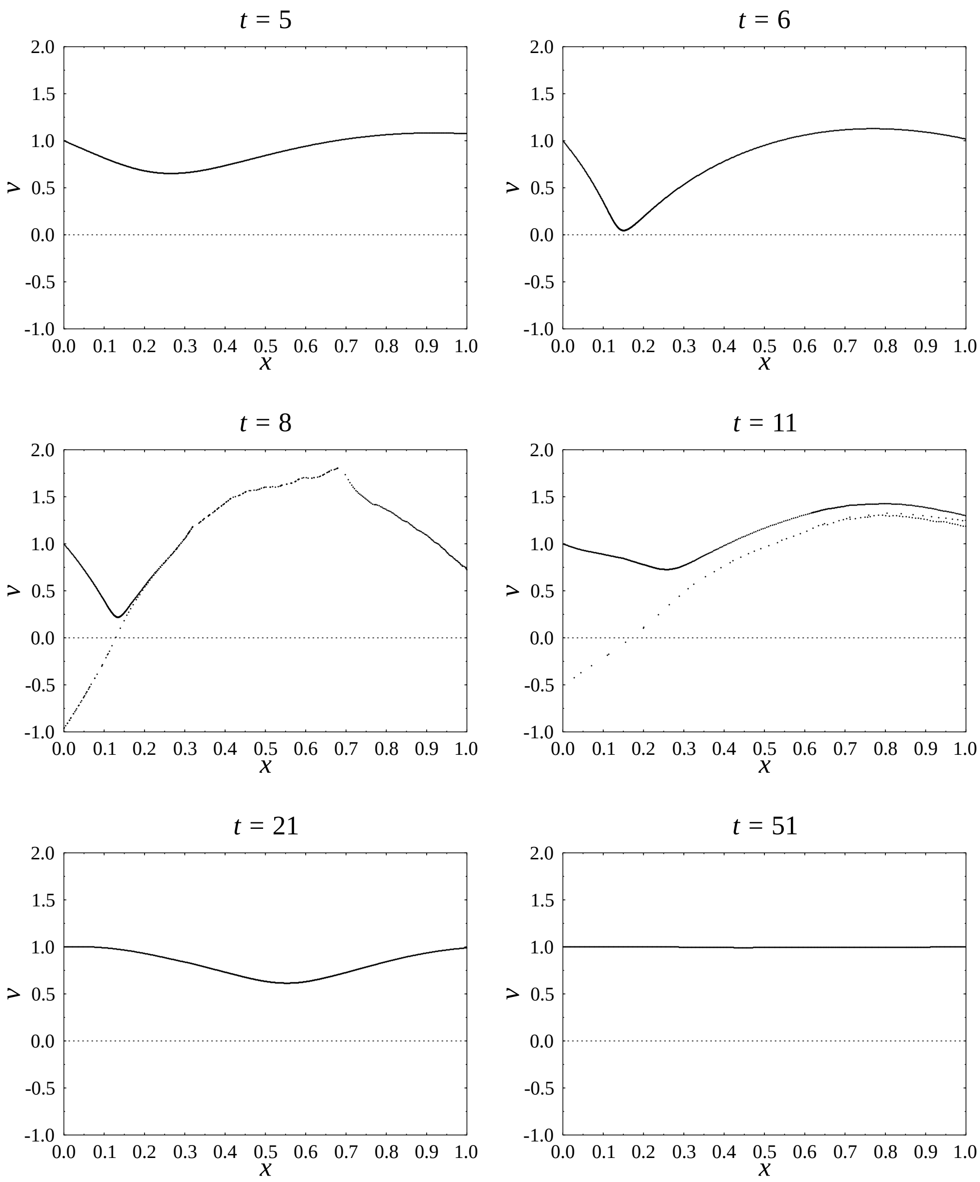

FIG. 4. Phase space plots in the case of suppressing virtual cathode oscillations by nonlinear feedback. Shown is the velocity $v(x)$ at different times.

If the system is near the unstable homogeneous equilibrium, we have shown numerically that control can be achieved by applying linear feedback to stabilize the homogeneous solution. Unfortunately, in experiments the initial conditions are generally far away from the homogeneous case.

In the situation where the linear control fails we applied nonlinear control instead. It can be easily implemented here: The homogeneous solution is a hyperbolic fixed point with a one–dimensional unstable manifold. Theory states [3], that the long time dynamics of the controlled system is then determined by an equation of motion which is also one–dimensional. In turn, this means that any scalar system output depending linearly on the amplitude of the unstable mode contains enough information to control the system.

To control virtual cathode oscillations we choosed the (dimensionless) net charge $Q(t) = \int \rho(x,t)\mathrm{d}x + 1$ as the scalar output signal. This choice is rather arbitrary. In the next section we show that other system variables, like charge density or velocity, will also work. The same is valid for the control signal. Here, we choosed the electron charge density at the boundary $\rho(0,t)$. Our nonlinear control law then becomes

$$\rho(0,t) = \rho_0 + h_1 Q(t) + h_2 Q(t)^2 \quad . \tag{3.2}$$

By optimizing the coefficients h_1 and h_2 we determined $h_1 = -0.038/q_c$ and $h_2 = 0.3/q_c$, where q_c is the charge of one macro–particle. This control law stabilizes the system in the presence of virtual cathode oscillations. In our simulation we used a value of $\alpha = 3\pi/2$, where the growth rate of the unstable mode has its maximum. Stabilization can be recognized in the phase space plots of Fig. 4: At time $t = 5$ the system is near the equilibrium $v(x) = 1$, but the unstable mode already has grown significantly. At time $t = 6$ a virtual cathode forms, which is indicated by the velocity becoming nearly zero in front of the cathode at $x \approx 0.14$. This leads to an accumulation of electrons generating a high negative charge density, so that parts of the electron beam are reflected to the cathode ($t = 8$). If the system is left to itself, these reflections induce a rarefaction wave which resolves the virtual cathode. Then the process starts again, leading to an oscillation. Here, we activated our nonlinear control at $t = 10$. At time $t = 11$ the system already comes close to the homogeneous state. At time $t = 21$ it is back in the hydrodynamic regime. Then the amplitude of the formerly unstable mode slowly decays, and at time $t = 51$ the system is in the now stabilized homogeneous state.

In the simulations we used a grid spacing of $\Delta x = 0.005$ and a particle number of $N \approx 500$. Thus, the charge of a macro–particle is $q_c = 0.002$. All values are given in dimensionless units. The same procedure can be applied in the next interval of purely exponential growth ($3\pi < \alpha < 4\pi$). The coefficients for, e.g., $\alpha = 11$ have then the values $h_1 = -0.058/q_c$ and $h_2 = 0.5/q_c$. This offers the important opportunity to approach the regime of oscillatory instability from above, with the well defined homogeneous state as initial condition. We already noticed that this possibility is important in experimental situations. In the following we shall discuss how the chaotic oscillations (which occur in that regime) can be controlled.

C. Controlling chaotic oscillations

It is often argued that the OGY approach [1] is very expensive in terms of computational costs and thus one is tempted to prefer other methods like, e.g., time–delay–feedback autosychronisation [21]. The reason is that the OGY–law depends in principle on the complete system state $\mathbf{x}_n$ (in our case it is infinite dimensional), although it is projected on the unstable manifold. This suggests that one has to reconstruct the phase space in the neighborhood of the unstable fixed point to some degree. In practice it is, however, often sufficient to use a scalar system output, as we will see now.

Despite its fractal nature a chaotic attractor extends mainly along the unstable manifold in the neighborhood of a hyperbolic fixed point. In the present case the fixed point (periodic orbit) has a one–dimensional unstable manifold. Thus, as was the case for the homogeneous solution, a scalar system output will be sufficient for the description of the system state. Theory states that this remains valid in the controlled situation too, which is a simple consequence of the reduction principle. The control law (3.1) can then be simplified to

$$\Delta p = \frac{\lambda_u}{\lambda_u - 1} \frac{\rho_n - \rho_f}{\mathrm{d}\rho_f/\mathrm{d}p} \quad , \tag{3.3}$$

where ρ_n denotes the scalar output signal at "time" n, and ρ_f is its value according the the fixed point. Keeping in mind that the factor $\lambda_u/(\lambda_u - 1)/(\mathrm{d}\rho_f/\mathrm{d}p)$ represents the strength of the feedback, this shows that also the OGY–method can be realized by trial and error. Here, one has to vary only two parameters, namely the feedback strength and the expected fixed point value ρ_f. From this point of view we see no reason why time–delay–feedback should be prefered, since it also needs the variation of two paramters, the delay time and the feedback strength. Beyond that, its range of applicability is restricted to certain values of λ_u [3], such that only orbits with a finite torsion may be stabilized. This means, e.g., that time–delay–feedback cannot be used to control the homogeneous solution.

The first step in controlling the chaotic osciallations is the definition of a Poincaré map. This reduces the time–continous flow to a discrete mapping where the control law is directly applicable. A reduction is achieved by triggering a measurement of the velocity at $x = 1/4$ whenever the deviation of the charge density from the homogeneous value ρ_0 at $x = 1/4$ passes through zero towards positive values. This offers us a time series of measurements at the Poincaré times. By plotting values at "time" $n+1$ against values at "time" n we gain a so called return map shown in Fig. 5 for an α–value of 8.951 in the chaotic regime. From here we easily determine the fixed point value $v_f = 0.04975$ of the desired orbit, lying on the bisection of an angle, and the unstable eigenvalue $\lambda_u = -1.90$ given by the gradient at the fixed point (dashed line in Fig. 5).

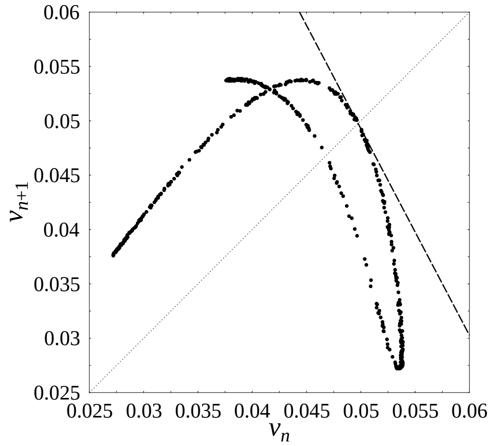

FIG. 5. Return map for the scalar system output at Poincaré times.

The fixed point shift depending on changes of the control parameter – now we change the value of v at the left boundary by Δv – can be determined by repeating the numerical experiment for a slightly different value of the control parameter. We choosed $\Delta v = 0.001$ and got $v_f = 0.05105$. Thus, we gained all the information needed for control.

In a typical numerical simulation we started with an uncontrolled system until the trajectory has settled down on the chaotic attractor. After a time, e.g. $t = 600$, we activated control. Then we waited until the trajectory comes close to the desired fixed point, e.g. until $|v_n - v_f| < 0.001$. In the present example this happend at $t = 649.413$. Now the control law was activated, and the system remained on the (now) stable limit cycle. The time series looks pretty much like the ones in simpler systems, like the logistic or Henón map (see e.g. [1]). Therefore we will not present them here. Much more interesting is the structure of the Fourier spectra of output of the continuous system, since it gives us the important information about the coherence of the generated microwaves.

Fig. 6 shows the Fourier spectrum of the scalar output signal $\rho(x = 1/4, t)$ in the uncontrolled case. Although it is slightly peaked around $\omega \approx 1.5$, it shows a broad band structure which is characteristic for any chaotic system.

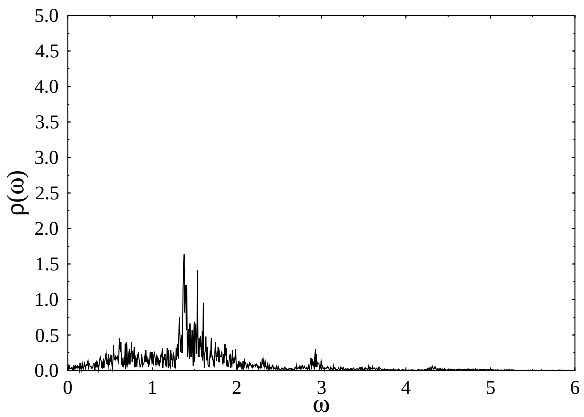

FIG. 6. Fourier spectrum of the scalar output signal in the uncontrolled case.

If we activate control, the Fourier spectrum changes dramatically. As can be seen from Fig. 7, the spectrum has now a large peak at $\omega \approx 1.5$, which is in very good agreement with the theoretical value $\omega = 1.4842$ given by center manifold theory. Since the limit cycle is a nonlinear oscillation, the spectrum also shows peaks at higher harmonics decaying exponentially.

Similar results have been produced by the application of time–delay–feedback. Because of its restriction to controlling the chaotic oscillations only, this procedure seems not to be the most useful one for the Pierce diode. Important is the fact that it is possible to optimize the feedback strength in such a way that the total energy fed into the control signal is minimized. One may economize 80% of the energy used when applying the OGY–law. Further 16% can be saved by the use of noise reduction techniques that will be discussed elsewhere.

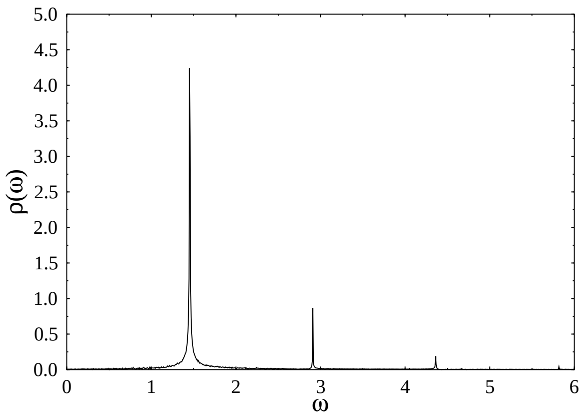

FIG. 7. Fourier spectrum of the scalar output signal in the controlled case.

IV. SUMMARY AND DISCUSSION

In this paper we have applied controlling techniques to the Pierce diode. The latter can be considered as a paradigm of a bounded plasma device. We used nonlinear control laws and considered both, the kinetic as well as hydrodynamic regime. The combination of various techniques and aspects allowed us to get a clear insight into the nonlinear dynamics close to the onset of both, the classical Pierce instability as well as the so called oscillatory instability. It turned out that virtual cathode oscillations should be controlled first if one aims to propose a broad controlling which will be robust enough also for experimental applications. We succeeded on suppressing the virtual cathode oscillations. That opened the route to a meaningful controlling of oscillatory states. As we have explained, the oscillatory instability leads, after a Hopf bifurcation, via period doubling to chaotic states. In the latter, unstable periodic orbits exist. Periodic orbits of an infinite–dimensional system were successfully controlled leading to pure oscillations on the microwave frequency domain. Besides possible technical aspects we would like to emphasize the point that this is one of the successful controls of chaotic states of relatively complex systems (compared, e.g., to discrete maps). This shows again that the pioneering idea of Ott, Grebogi and Yorke [1] has an enormous potential for applications.

Recently we learned that independent from our work Krahnstöver and coworkers [22] developed and successfully applied more experimentally motivated ideas to controlling the chaotic oscillations in the hydrodynamic regime. They use an external electric potential difference as control parameter. We hope that all these results will stimulate further numerical and experimental efforts aimed at improving the control of bounded low temperature plasmas.

ACKNOWLEDGMENTS

This work was performed under the auspices of the Sonderforschungsbereich 191.

---

[1] E. Ott, C. Grebogi, and J. A. Yorke, *Phys. Rev. Lett.* **64** (1990) 1196.
[2] J. P. LaSalle, *The stability and control of discrete processes*, Springer–Verlag, New York, 1986.
[3] H. Friedel, R. Grauer, and C. Marliani, *Phys. Lett. A* **236** (1997) 45.
[4] J. R. Pierce, *J. Appl. Phys.* **15** (1944) 721.
[5] L. Tonks and I. Langmuir, *Phys. Rev.* **33** (1929) 195.
[6] S. Kuhn, *Contrib. Plasma Phys.* **34** (1994) 495.
[7] J. R. Cary and D. S. Lemons, *J. Appl. Phys.* **53** (1982) 3303.
[8] M. Hörhager and S. Kuhn, *Phys. Fluids B* **2** (1990) 2741.
[9] E. N. Lorenz, *J. Atmos. Sci.* **20** (1963) 130.
[10] J. Carr, *Applications of center manifold theory*, Springer, New York, 1981.
[11] S. Chow and J. Hale, *Methods of Bifurcation Theory*, Springer, New York, 1982.
[12] R. Grauer, *Physica D* **35** (1989) 107.
[13] H. Friedel, *Dynamische Kontrolle chaotischer Zustände in Niedertemperaturplasmen*, PhD thesis, Heinrich–Heine–Universität Düsseldorf, 1997.
[14] W. S. Lawson, *Phys. Fluids B* **1** (1989) 1493.
[15] R. Benzi, A. Sutera, and A. Vulpiani, *J. Phys. A* **14** (1981) L453.
[16] B. B. Godfrey, *Phys. Fluids* **30** (1987) 1553.
[17] R. J. LeVeque, *Numerical methods for conservation laws*, Birkhäuser, Stuttgart, 1990.
[18] H. Yoshida, *Phys. Lett. A* **150** (1990) 262.
[19] C. K. Birdsall and A. B. Langdon, *Plasma Physics Via Computer Simulation*, McGraw–Hill, New York, 1985.
[20] H. Friedel, R. Grauer, and C. Marliani, *J. Comp. Phys.* **134** (1997) 190.
[21] K. Pyragas, *Phys. Lett. A* **170** (1992) 421.
[22] N. Krahnstöver, T. Klinger, F. Greiner, and A. Piel, *private communication*.